The *shh* limb enhancer is activated in patterned limb regeneration but not in hypomorphic limb regeneration in *Xenopus laevis*

Reimi Tada[1,*], Takuya Higashidate[2,*], Takanori Amano[3], Shoma Ishikawa[1], Chifuyu Yokoyama[1], Saki Nara[1], Koshiro Ishida[1], Akane Kawaguchi[4,#], Haruki Ochi[5], Hajime Ogino[6], Nayuta Yakushiji-Kaminatsui[7], Joe Sakamoto[8], Yasuhiro Kamei[8,9], Koji Tamura[2], and Hitoshi Yokoyama[1‡].

Affiliation: [1]Department of Biochemistry and Molecular Biology
Faculty of Agriculture and Life Science, Hirosaki University
3 Bunkyo-cho, Hirosaki, Aomori 036-8561, Japan.
[2]Department of Ecological Developmental Adaptability Life Sciences,
Graduate School of Life Sciences, Tohoku University,
Aramaki-Aza-Aoba 6-3, Aoba-ku, Sendai 980-8578, Japan.
[3]Next Generation Human Disease Model Team
RIKEN BioResource Research Center
3-1-1 Koyadai, Tsukuba, Ibaraki, 305-0074, Japan
[4]Graduate School of Biological Sciences, Nara Institute of Science and Technology (NAIST), Ikoma, Nara, Japan.
[5]Institute for Promotion of Medical Science Research, Faculty of Medicine, Yamagata University, Yamagata 990-9585, Japan.
[6]Amphibian Research Center / Graduate School of Integrated Sciences for Life, Hiroshima University, 1-3-1 Kagami-yama, Higashi-Hiroshima, Hiroshima 739-8526, Japan.
[7]RIKEN Center for Integrative Medical Sciences (IMS)
1-7-22 Suehiro-cho, Tsurumi-ku, Yokohama 230-0045, Japan
[8] Laboratory for Biothermology, National Institute for Basic Biology, Myodaiji, Okazaki, Aichi 444-8585, Japan
[9]Department of Basic Biology in the School of Life Science of the Graduate University for Advanced Studies (SOKENDAI), Okazaki,

Aichi 444-8585, Japan
[#]Present address: Molecular Life History Laboratory, Department of Genomics and Evolutionary Biology, National Institute of Genetics, Japan
*These authors contributed equally to this work.

Running Title: *shh* enhancer in limb regeneration

Key words: limb regeneration; *shh*; long-range enhancer; *Xenopus*; regenerative capacity

Summary statement: We visualized the activity of a limb-specific enhancer of *shh* in the regenerating limb of an amphibian, *Xenopus*: it correlates with the capacity for regeneration of a well-patterned limb.

[‡]Author for correspondence:
Hitoshi Yokoyama
Department of Biochemistry and Molecular Biology
Faculty of Agriculture and Life Science, Hirosaki University
3 Bunkyo-cho, Hirosaki, Aomori 036-8561, Japan.
E-mail: yokoyoko@hirosaki-u.ac.jp
Phone: +81-172-39-3773
FAX: +81-172-39-3773

ORCID ID
Reimi Tada: 0000-0003-4474-1372
Takanori Amano: 0000-0002-0213-4745
Shoma Ishikawa: 0000-0002-6688-0288
Chifuyu Yokoyama: 0000-0002-7476-7496
Saki Nara: 0000-0003-2565-8944
Koshiro Ishida: 0000-0001-6443-4033

Haruki Ochi: 0000-0002-0088-581X
Hajime Ogino: 0000-0003-2707-2330
Nayuta Yakushiji-Kaminatsui: 0000-0001-7324-1161
Yasuhiro Kamei: 0000-0001-6382-1365
Koji Tamura: 0000-0002-1956-2826
Hitoshi Yokoyama: 0000-0003-4821-9506

ABSTRACT

Xenopus young tadpoles regenerate a limb with the anteroposterior (AP) pattern, but metamorphosed froglets regenerate a hypomorphic limb after amputation. The key gene for AP patterning, *shh*, is expressed in a regenerating limb of the tadpole but not in that of the froglet. Genomic DNA in the *shh* limb-specific enhancer, MFCS1 (ZRS), is hypermethylated in froglets but hypomethylated in tadpoles: *shh* expression may be controlled by epigenetic regulation of MFCS1. Is MFCS1 specifically activated for regenerating the AP-patterned limb? We generated transgenic *Xenopus laevis* lines that visualize the MFCS1 enhancer activity with a GFP reporter. The transgenic tadpoles showed GFP expression in *hoxd13*- and *shh*-expressing domains of developing and regenerating limbs, whereas the froglets showed no GFP expression in the regenerating limbs despite having *hoxd13* expression. Genome sequence analysis and co-transfection assays using cultured cells revealed that Hoxd13 can activate *Xenopus* MFCS1. These results suggest that MFCS1 activation correlates with regeneration of AP-patterned limbs and that re-activation of epigenetically inactivated MFCS1 would be crucial to confer the ability to non-regenerative animals for regenerating a properly patterned limb.

INTRODUCTION

Among tetrapods, only urodele amphibians (newts and salamanders) can regenerate an amputated limb throughout their life cycles (Han et al., 2005; Joven et al., 2019; Otsuki and Tanaka, 2022). In *Xenopus laevis*, a tadpole can regenerate its limbs prior to metamorphosis, but it loses regenerative capacity gradually as metamorphosis proceeds (Dent, 1962; Muneoka et al., 1986). The froglet, a young post-metamorphosis adult, regenerates only a spike-like structure after limb amputation (Dent, 1962; reviewed in Suzuki et al., 2006): the spike lacks the anteroposterior (AP) pattern. In the limb formation process, *sonic hedgehog* (*shh*) is expressed posteriorly in the limb bud and serves as the key gene for the AP axis formation (Riddle et al., 1993; Harfe et al., 2004). *shh* is also expressed in the posterior part of a regenerating limb (blastema) in urodeles (Imokawa and Yoshizato, 1997; Torok et al., 1999). In *Xenopu*s, *shh* is expressed posteriorly in the limb blastema of a tadpole (Endo et al., 1997) but is not expressed in the blastema of a froglet limb (Endo et al., 2000; Yakushiji et al., 2007). Treatment with a Hedgehog inhibitor results in hypomorphic limb regeneration in both a *Xenopus* tadpole and an axolotl (Roy and Gardiner, 2002; Satoh et al., 2006). These results suggest that *shh* re-expression correlates with the limb regenerative capacity: whether a limb regenerates with the AP pattern or not.

Genetic studies in mice have revealed that a long-range enhancer called MFCS1 (mammal-fish-conserved-sequence 1), also called ZRS or Rr29, regulates limb-specific *Shh* expression (Lettice et al., 2003; Sagai et al., 2004). In transgenic (Tg) mouse, MFCS1 with a minimal promoter drives *lacZ* expression in the posterior part of a limb bud (Lettice et al., 2003). Depletion of a large part of MFCS1 results in limb-specific loss of *shh* expression and in loss of the AP polarity of a limb (Sagai et al., 2005). The activity of MFCS1 is positively regulated by Hoxd13 and ETS transcription factors, downstream factors of FGF signaling in a mouse limb bud that directly bind to MFCS1 (Capellini et al., 2006; Lettice et al., 2012). In amphibian limbs, the methylation level of genomic DNA in MFCS1 is high in the limbs of a *Xenopus* froglet, while the level is low to medium in the limbs of a *Xenopus* tadpole, an axolotl and a Japanese newt (Yakushiji et al., 2007). These findings strongly suggest that epigenetic inactivation of MFCS1 leads to the shutdown of *shh* expression that results in hypomorhic limb regeneration without the AP

120 pattern in a froglet. The importance of MFCS1 for limb regeneration is further supported
121 by the partial deletion of MFCS1 in an Iberian ribbed newt: it resulted in reduction in *shh*
122 expression (Suzuki et al., 2018). However, the spatio-temporal activation pattern of
123 MFCS1 has not been visualized in regenerating limbs of amphibians.

124 Here, we succeeded in visualizing the spatio-temporal pattern of MFCS1
125 activation in regenerating limbs by establishing Tg *Xenopus laevis* lines carrying a GFP
126 linked to MFCS1 (MFCS1-GFP). Expression patterns of MFCS1-GFP were overlapped
127 with those of *shh* both in limb development and limb regeneration. MFCS1-GFP
128 expression was specifically localized in the regenerating limb of a young tadpole but was
129 not found in the regenerating froglet limb. We revealed that the DNA methylation level
130 of exogenous MFCS1 of the transgene as well as that of endogenous MFCS1 in the limb
131 were higher in the froglet than in the tadpole. Our results suggest that MFCS1 is activated
132 in limb regeneration with the AP pattern but is inactivated in hypomorphic limb
133 regeneration after metamorphosis when MFCS1 has a higher DNA methylation status
134 than that in tadpole stages.

135

136 RESULTS AND DISCUSSION

137 MFCS1-GFP expression localizes in the posterior mesenchyme of a developing limb 138 bud

139 To visualize the MFCS1 activity, we generated a transgene construct containing GFP
140 downstream of a *Xenopus shh* promoter (Yakushiji et al., 2007) and MFCS1 sequences
141 (Fig. 1A). We generated transgenic *X. laevis* containing this transgene named
142 "*Xla.Tg(Xtr.shh:GFP)*^{Tamura}" (according to the Xenbase nomenclature). For highlighting
143 the involvement of MFCS1 enhancer, we hereafter refer to this Tg as MFCS1-GFP. We
144 observed the GFP pattern in G0 founders. Since *shh* is most prominently expressed
145 posteriorly in a limb bud at stage 51-52 (Endo et al., 1997; Fig. 1B), we firstly observed
146 at stage 51-52 (Nieuwkoop and Faber, 1994). GFP was found in the posterior part of the
147 limb bud in at least eleven independent G0 individuals and the fluorescence gradually
148 diminished after stage 52. Thus, we considered that MFCS1-GFP expression reflects the
149 activity of the MFCS1 enhancer. We established two independent lines by mating selected
150 GFP-expressing founder animals with wild-type frogs (Table S1). About 50% of the N1

individuals of line 2 as well as the N1 and N2 individuals of line 1 were GFP-positive in limb buds, presumably being inherited in a Mendelian manner. Limb buds of both line 1 and line 2 at stage 51-52 also showed GFP expression in the posterior part (Fig. 1C, C' and Fig. S1A, A'). In the following experiments, we used GFP-positive individuals of line 1 (N1 or N2) and line 2 (N1).

Confocal imaging revealed GFP localization in the posterior mesenchyme of the limb bud at stage 51-52 (Fig. 1D, E and Fig. S1B, C). In limb development, GFP was firstly observed at stage 50 in a limb bud (Fig. 1F, F' and Fig. S1D, D'). This observation is consistent with the initial weak *shh* expression detected at stage 50 by *in situ* hybridization (Endo et al., 1997). GFP expression became strongest at stages 51-52 and the fluorescence was more posteriorly polarized by stage 52 (Fig. 1G, G', H, H' and Fig. S1E, E', F, F'). At stage 53, the fluorescence was weaker than that at stage 52 (Fig. 1I, I' and Fig. S1G, G'). Finally GFP expression was almost undetectable at stage 54 (Fig. 1J, J' and Fig. S1H, H'). These observations were, in principle, consistent with the spatio-temporal *shh* expression patterns (Endo et al., 1997), while the GFP expression appeared to be broader than that of *shh* expression. We concluded that the MFCS1-GFP expression pattern in the Tg lines mostly visualizes the activity of the endogenous MFCS1 enhancer in a developing limb bud.

MFCS1-GFP expression predicts the AP duplication of a limb bud

To further examine whether MFCS1-GFP expression correlates with limb morphogenesis along the AP axis, we conducted a 180° rotation experiment on limb buds of Tg (line 1) tadpoles (Fig. 2A). Cameron and Fallon (1977) found limb duplication along the AP axis after rotation of the distal limb bud tips 180° in *X. laevis*. Endo et al. (1997) repeated this experiment and found that ectopic *shh* expression was induced in the posterior region of the graft and stump. To test the correlation between MFCS1 enhancer activity and limb duplication, we repeated this experiment (Fig. 2). Consistent with the preceding results in control limb buds without rotation, showing only faint ectopic *shh* expression (Endo et al., 1997), the control limb buds (ten of 12 samples) did not show GFP expression and did not result in limb duplication (Fig. 2B, C). In contrast, the 180° rotated limb buds (eight of 11 samples) showed ectopic induction of GFP expression in the posterior part of the graft and finally formed duplicated limbs along the AP axis (Fig. 2D-G). These

183 results (summarized in Table S2) suggest that ectopic induction of MFCS1 activity is
184 closely related to ectopic *shh* expression and subsequent limb duplication along the AP
185 axis, further suggesting that MFCS1-GFP expression reflects the endogenous *shh*
186 enhancer activity.
187
188 **MFCS1 is activated in a blastema that regenerates a limb with the AP pattern.**
189 To examine whether MFCS1 is activated in limb regeneration with the AP pattern, we
190 amputated a stage 54 limb bud at the ankle level: this amputation results in almost
191 complete limb regeneration (Muneoka et al., 1986). By this stage, *shh* and MFCS1-GFP
192 expression in a limb bud have become almost undetectable (Fig. 1 and Fig. S1) (Endo et
193 al., 1997). At 4 days post amputation (dpa), GFP was observed broadly in the regenerating
194 blastema (Fig. 3R and Fig. S2B-B''), indicating that MFCS1 is re-activated in the
195 blastema that regenerates a well-patterned limb.
196 MFCS1-GFP expression was distributed throughout the blastema and not
197 localized posteriorly. It became stronger at 6 dpa (Fig. S2C-C''), then the expression
198 gradually diminished (Fig. 3S, T and Fig. S2). *shh* expression was restricted posteriorly
199 in a blastema at 4 dpa (Fig. 3E). Based on these results, we judged that MFCS1-GFP
200 expression is distributed broadly in regenerating blastemas and that the temporal
201 expression pattern of MFCS1-GFP coincidences with that of *shh* expression, while the
202 spatial MFCS1-GFP expression pattern is wider than the *shh*-expressing domain.
203 MFCS1-GFP signal in the regenerating blastema of a young tadpole suggests that MFCS1
204 is re-activated in a regenerating limb with the AP pattern formation when *shh* is
205 expressed: *shh* expression in the regenerating limb as well as in the developing limb
206 seems to be regulated by the common enhancer, MFCS1.
207
208 **MFCS1-GFP expression pattern correlates with the pattern of *hoxd13* in a tadpole**
209 Hoxd13 and FGF downstream factors, ETS transcription factors, positively regulate the
210 MFCS1 enhancer in mice (Capellini et al., 2006; Lettice et al., 2012). We examined *dusp6*
211 (*mkp3*) and *hoxd13* expression as indicators of positive upstream regulators of MFCS1.
212 *dusp6* expression is induced by FGF signaling (Eblaghie et al., 2003; Kawakami et al.,
213 2003) and especially reflects the activity of ETS transcription factors (Ekerot et al., 2008).
214 We chose a stage 51 limb bud and a 4 dpa blastema of a tadpole in which the limb bud

215 was amputated at the ankle level at stage 54 as representatives of developing and
216 regenerating limbs, respectively: both initiate prominent *shh* expression in the posterior
217 side (Fig. 3E, I). In a developing limb bud, *dusp6* is expressed broadly and strong
218 expression is seen especially in the apical mesenchyme (Fig. 3K). *hoxd13* is expressed in
219 the posterior mesenchyme (Fig. 3L) and its expression domain is wider than the *shh*-
220 expressing domain (Fig. 3I). The posterior mesenchymal region of a limb bud is positive
221 for both *dusp6* and *hoxd13* and the double positive region coincides with the fluorescence
222 of MFCS1-GFP (Fig. 1C', D, G') and *gfp* transcript (Fig. 3J) patterns. The *gfp* transcript
223 was not detected in line 2 limb bud samples (n=0/6) but was detected in line 1 limb bud
224 samples (n=10/10) by *in situ* hybridization, suggesting that line 1 has stronger transgene
225 expression than that of line 2. The coincidence between upstream regulators and MFCS1-
226 GFP expression was clearer in a regenerating limb: *dusp6* (Fig. 3G) and *hoxd13* (Fig. 3H)
227 were strongly expressed in whole region of a blastema. MFCS1-GFP expression (Fig.
228 3R) and *gfp* transcript (Fig. 3F) are robustly distributed in the entire blastema, while *shh*
229 expression is restricted posteriorly (Fig. 3E). Therefore, the MFCS1-GFP expression
230 domain is larger than the *shh* expression domain, especially in a regenerating limb.
231 Transcriptional repression by a silencer or defined regulation of chromatin
232 conformational change resulting in the proximity of MFCS1 and the *shh* promoter
233 (Amano et al., 2009) may further restrict endogenous *shh* expression to the posterior edge
234 of the blastema. Even though *shh* expression is spatially narrower than the GFP
235 expression pattern, the expression pattern of MFCS1-GFP covers the *shh*-expressing
236 domain and coincides with the expression domains of upstream regulators represented by
237 *hoxd13* and *dusp6*.
238

239 **MFCS1 is inactive in a limb blastema of a metamorphosed froglet despite *hoxd13***
240 **expression**

241 A limb of a metamorphosed froglet does not express *shh* after amputation, and amputation
242 results in regeneration of a spike, while an amputated limb of a froglet forms a
243 regeneration blastema (Endo et al., 2000; Suzuki et al., 2006; Yakushiji et al., 2007).
244 Hypermethylated genomic DNA at the MFCS1 strongly suggested that this enhancer is
245 inactivated in a froglet limb: it implies transcriptional inactivation of *shh* in the limb
246 (Yakushiji et al., 2007). To examine whether inactivation of the enhancer occurs after

247 metamorphosis, we examined MFCS1-GFP expression in limb regeneration of a froglet.
248 From the early to the late stage, no specific GFP was observed in the blastema (Fig. 3M-
249 P and Fig. S3). Therefore, we conclude that MFCS1 is inactivated completely or is much
250 more inactive in the blastema of a froglet limb than in that of a young tadpole.

251 We then examined expression of upstream regulators of MFCS1. By 10 dpa, an
252 amputated limb of a froglet forms a cone-shaped blastema and it already starts expressing
253 *fgf-8*, *fgf-10*, *msx1*, and *hand2* (Suzuki et al., 2005; Yakushiji et al., 2007). In addition,
254 Yakushiji et al. (2007) reported hypermethylation of genomic DNA at the MFCS1 in a
255 limb blastema at 10 dpa in a froglet. Therefore, we chose the blastema at 10 dpa and
256 examined gene expression. At 10 dpa, *hoxd13* was broadly expressed (Fig. 3D). *dusp6*
257 was also expressed (Fig. 3C), while no *shh* (and *gfp*) expression was detected in the
258 blastema as Yakushiji et al. (2007) reported (Fig. 3A, B). The expression of *hoxd13* and
259 *dusp6* in a froglet blastema suggests that upstream regulators of MFCS1 (5' Hoxd and
260 ETS transcription factors) as well as *hand2* (Yakushiji et al., 2007) are not absent in the
261 froglet blastema. Thus, MFCS1 in a froglet limb appears to be unable to respond to
262 positive regulators represented by Hoxd13.
263

264 **Higher DNA methylation level of MFCS1 may inactivate the enhancer's**
265 **responsiveness to Hoxd13 in a froglet limb**

266 A local alignment of the highly conserved sequences revealed multiple putative Hox-
267 binding motifs in MFCS1 (Fig. 4A, see also Fig. S4). To confirm the potential
268 responsiveness of MFCS1, MFCS1-*shh* promoter-*luc2* or MFCS1-minP-*luc2* reporter
269 constructs (Fig. 4A) were co-transfected with the gene expression constructs into NIH3T3
270 cells. The reporter activities with MFCS1-*shh* promoter-*luc2* were significantly increased
271 with *Fgf2* (1.4-fold vs. mock), *Fgf4* (1.5-fold vs. mock), *Fgf8* (1.3-fold vs. mock), or
272 *Hoxd13* (2.3-fold vs. mock) (Fig. 4B). When the MFCS1-*luc2* was artificially methylated
273 by CpG methyltransferase in advance, the responsiveness to Hoxd13 was strongly
274 suppressed by ~260 fold (Fig. S5). Taken together with the highly methylated MFCS1 in
275 a *Xenopus* froglet limb (Yakushiji et al., 2007), this result raises the possibility that DNA
276 methylation of MFCS1 inactivates its responsiveness to Hoxd13.

277 To further examine whether a high methylation level of MFCS1 exerts a
278 suppressive effect on gene expression, we investigated the methylation status of MFCS1

279 as the transgene in MFCS1-GFP Tg tadpoles and froglets. Within an MFCS1 highly
280 conserved sequence in amphibians, there are nine CpG sites in *X. tropicalis* and *X. laevis*
281 (Fig. S6). Firstly, we examined DNA methylation status of MFCS1 in wild-type tadpoles
282 and froglets by bisulfite sequencing as reported by Yakushiji et al. (2007) and obtained
283 consistent results: Young tadpoles have a lower methylation (26.3%) and froglets have a
284 higher methylation level (87.2%) in the limbs (Fig. 4C). We then examined the
285 methylation level of MFCS1 as the transgene in MFCS1-GFP Tg (line 1). Again, froglet
286 limbs have a higher methylation level (17.2%) than that in limb buds of young tadpoles
287 (2.6%) (Fig. 4C). After limb amputation in a froglet and after completion of spike
288 regeneration, a higher methylation level than that in tadpoles was still found in the Tg
289 regenerates (line 1, 14.4%) (Fig. S7). MFCS1 as the transgene was susceptible to
290 methylation to some extent also in line 2 (Fig. S7). Although the basal methylation level
291 differs between endogenous MFCS1 and transgene MFCS1, the increase in the
292 methylation level of the transgene MFCS1 after metamorphosis also correlated with the
293 ontogenetic inactivation of gene expression under control of the enhancer.
294

295 **Conclusions**

296 In this study, we visualized MFCS1 activity in limb regeneration of an amphibian.
297 MFCS1 is re-activated in the regenerating blastema for a patterned limb in a young
298 tadpole but not in the blastema for a hypomorphic limb in a froglet. MFCS1 seems to be
299 activated by Hoxd13 in a tadpole but unable to respond to Hoxd13 in a froglet. An
300 ontogenetic increase in the MFCS1 methylation may block the function of Hoxd13 (and
301 other positive regulators) as a transcriptional activator(s) to the enhancer so that
302 transcription of a gene under the enhancer is inactivated (Fig. 4D). For improvement of
303 regenerative capacity in a froglet limb by re-activation of *shh* expression, removal of
304 epigenetic silencing of MFCS1 would be important. The combinational application of an
305 inhibitor of DNA methyltransferase and a histone deacetylase inhibitor stimulated *shh*
306 expression in cultured limb blastema cells of a froglet (Yakushiji et al., 2009), suggesting
307 that application of such reagents could be hopeful if the condition is optimized *in vivo*.
308 As an alternative approach, CRISPR-based epigenome editing that removes DNA
309 methylation (e.g., Nuñez et al., 2021) may be effective. In these approaches, the MFCS1-
310 GFP Tg line would be useful for evaluation: The enhancer activation is easily detected

311 by GFP and it would thus be possible to screen chemicals that remove epigenetic silencing
312 of the enhancer in a large scale. If regeneration of a well-patterned limb is induced in a
313 froglet by re-activation of MFCS1, it would be a precious model case for recovery of
314 organ-level regeneration in non-regenerative higher vertebrates by manipulating
315 epigenetics.
316

317 # MATERIALS AND METHODS

318 **Transgene construction and *in situ* hybridization**

319 A 3,164-bp MFCS1 enhancer sequence was amplified from *Xenopus tropicalis* genomic
320 DNA prepared from a Nigerian line with primers (XtMFCS1-Fw and Xt-MFCS1-Rv;
321 Table S3). The PCR product was cloned into the pCRII-TOPO vector (Invitrogen) and
322 sequenced. The *Xenopus laevis shh* promoter (Yakushiji et al., 2007) was cloned into a
323 reporter construct that contains an EGFP expression cassette. Then the MFCS1-*shh*
324 promoter-*egfp* was generated by inserting the 3,164-bp MFCS1 enhancer sequence
325 upstream of the *shh* promoter (Fig. 1A). For synthesis of probes for *in situ* hybridization,
326 a *hoxd13* cDNA clone, BC080434, inserted in pCMV-SPORT6 was obtained from
327 Dharmacon. The *hoxd13*/ pCMV-SPORT6 plasmid was linearized with SalI and
328 transcribed with T7 RNA polymerase. DIG-labeled RNA probes of *hoxd13*, *shh* (Endo et
329 al., 1997), *gfp* (Hayashi et al., 2015) and *dusp6* (Gomez et al., 2005) were prepared
330 according to the protocol of the manufacturer (Roche). To prepare serial cryosections, the
331 specimens were fixed in MEMFA (0.1 M MOPS at pH 7.4, 2 mM EGTA, 1 mM $MgSO_4$,
332 3.7% formaldehyde) overnight at room temperature, embedded in OCT compound
333 (Sakura), and serially sectioned at 8-10 µm by a cryostat. *In situ* hybridization on frozen
334 sections was performed according to Yoshida et al. (1996) with slight modifications.
335 Sections were observed under an upright microscope (Olympus BX53) with an objective
336 lens (Olympus UPlan PLN 10X) and were photographed by a digital camera (Leica
337 DFC7000T).
338

339 **Animal husbandry and transgenesis in *Xenopus laevis***

340 Wild-type *Xenopus laevis* adult frogs were purchased from domestic animal venders,
341 Watanabe Zoushoku (http://www5d.biglobe.ne.jp/~zoushoku/top.htm) and Hamamatsu

342 Seibutsu Kyozai (http://www.h-seibutsu.co.jp/index.html). Founder (G0) MFCS1-GFP
343 Tg *Xenopus laevis* embryos were generated by a REMI technique (Kroll and Amaya,
344 1996) using oocyte extract instead of egg extract (Hirsch et al., 2002; reviewed in Ogino
345 and Ochi, 2009). MFCS1-GFP N1 Tg *Xenopus laevis* lines were obtained by crossing
346 sexually mature MFCS1-GFP G0 frogs with wild-type frogs. Tadpoles and froglets were
347 reared at 22–23°C in dechlorinated tap water. The rearing containers were cleaned daily,
348 and the tadpoles were fed powdered barley grass (Odani Kokufun, Japan or Yamamoto
349 Kanpoh, Japan). At stage 58 (Nieuwkoop and Faber, 1994), the feeding was ceased until
350 metamorphosis was completed. After metamorphosis, the froglets were fed dried tubifex
351 every other day. All surgery was performed under ethyl-3-aminobenzoate anesthesia, and
352 all efforts were made to minimize suffering. When tadpoles and froglets needed to be
353 euthanized, they were immersed in 0.05% ethyl-3-aminobenzoate (Tokyo Chemical
354 Industry, 886-86-2). When adult male frogs were sacrificed to excise their testes for
355 transgenesis, 2% ethyl-3-aminobenzoate dissolved in pure water was injected into the
356 intracardiac cavity (400 µg of ethyl-3-aminobenzoate/1 g of animal). After the male frog
357 was confirmed to be completely unconscious, its testes were excised with a blade, and
358 then the unconscious frog was put in a freezer for euthanization. All animal care and
359 experimentation procedures were conducted in accordance with the animal care and use
360 committee guidelines of Tohoku University (2015LsA-023) and Hirosaki University
361 (A15003, A15003-1).
362

363 **Observation of developing and regenerating limbs, limb amputation and 180°**
364 **rotation of a limb bud**

365 For observation of limb development and limb regeneration in tadpoles, we used hindlimb
366 buds since it is much easier to observe and to operate on hindlimb buds than forelimb
367 buds due to their size and accessibility. To observe the regenerating limb bud (blastema)
368 of a tadpole, tadpoles at stage 54 were anesthetized with 0.025% ethyl-3-aminobenzoate
369 and hindlimb buds were amputated using ophthalmologic scissors at the presumptive
370 ankle level (according to the outside view and a fate map by Tschumi, 1957). For
371 preparation of a 180° rotated limb bud, Nile Blue A particles were embedded into the
372 anterior side of the distal tip of a stage 53 hindlimb bud with a tungsten needle as the
373 reference point indicating the original AP axis of the graft according to Cameron and

Fallon (1977). Subsequently, the limb bud was amputated at the presumptive ankle level (Tschumi, 1957) and then the distal limb bud tip was rotated 180° (not rotated for control limbs) on the proximo-distal axis, returned to the stump, and fixed with tungsten pins according to Cameron and Fallon (1977) and Endo et al. (1997). After metamorphosis, the resulting limbs were fixed in 10% formalin in Holtfreter's solution and stained with 0.1% Alcian blue as previously reported (Yokoyama et al., 1998). Then digit identity was determined by the number of phalanges in association with the presence/absence of a claw (Cameron and Fallon, 1977). To observe the blastema of a froglet, froglets were anesthetized with 0.05% ethyl-3-aminobenzoate and then forelimbs were amputated through the distal zeugopodium with ophthalmologic scissors and the amputation surface was trimmed to be flat. For observation of limb regeneration in froglets, we used forelimbs since hindlimb amputation often results in drowning of the froglets.

Imaging of whole-mount limb samples

Tadpoles and froglets anesthetized with 0.025% or 0.05% ethyl-3-aminobenzoate were observed under a fluorescence stereomicroscope (Nikon SMZ18) with a 0.5x objective lens using a GFP longpass filter (if in a fluorescent view) and photographed by a digital camera (Olympus DP74 or DP73). For confocal microscopy (Fig. 1D, E and Fig. S1B, C), anesthetized tadpoles were each placed on a 35-mm glass-bottom dish (Iwaki, Japan) so that the dorsal surface of the hindlimb bud was tightly attached to the glass-bottom. The prepared samples were observed under an FV3000 confocal laser scanning microscope (Olympus) equipped with an Olympus UplanSApo 20× dry objective lens. Fluorescence between 500 nm and 600 nm was detected by a GaAsP photo multiplier tube. Optical-section images at approximately 60-80 μm in depth from the dorsal surface of the limb bud were photographed.

Genome sequence analysis

The 449-b genomic sequences corresponding to a conserved core region of human MFCS1 (hg38, chr7: 156,791,242－156,791,690) and its orthologous sequences in the mouse (mm39, chr5: 29,520,033–29,520,474), chicken (galGal6, chr2: 8,553,351–8,553,801), *X. tropicalis* (xenTro10, chr6: 17,346,249–17,346,700) and *X. laevis* (J-strain

405 10.1, Chr6L: 15,900,483–15,900,931) were downloaded from the UCSC Genome
406 Browser and Xenbase (Karolchik et al., 2003; Fortriede et al., 2020). These sequences
407 were aligned using MUSCLE (Edgar, 2004). Searches for potential transcription factor-
408 binding sites were performed with transcription factor-binding motifs collected from the
409 TRANSFAC and JASPAR databases (Wingender, 2008; Castro-Mondragon et al., 2022).
410 The *X. tropicalis* MFCS1 element used for our functional analyses contains a 12-
411 thymidine repeat in place of the 14-thymidine repeat underlined in the alignment (Fig.
412 4A, underlined). This difference may be because of a polymorphism between the strain
413 used for our study and that used for the genome sequencing project (Igawa et al., 2015).
414

415 **Reporter construction, cell culture and luciferase assay**

416 The highly conserved 998-bp core sequence of *Xenopus tropicalis* MFCS1 was amplified
417 by PCR with specific primers (Table S3) and inserted into the Acc65I and XhoI sites of
418 the pGL4.23 vector (Promega, E8411). Then the minimal promoter of the pGL4.23 vector
419 was replaced with a 486-bp sequence of *Xenopus laevis shh* promoter (Fig. 4A). It should
420 be noted that the 14-thymidine repeat in *X. tropicalis* MFCS1 sequence from the UCSC
421 Genome Browser (Fig. 4A, underlined) was shortened to a 12-thymidine repeat in the
422 transgene construct (Fig. S6) and the reporter construct for the luc assay. pGL4.74
423 containing the *Renilla* luciferase gene was used for normalization of reporter expression
424 (Promega, E6921). Coding sequences of mouse *Hoxd13*, *Fgf2*, *Fgf4* and *Fgf8* were cloned
425 into the pcDNA3.1 vector (ThermoFisher, V79020). NIH3T3 cell line (RCB2767) was
426 obtained from the RIKEN BioResource Research Center. NIH3T3 cells were maintained
427 in Dulbecco's modified Eagle's medium (ThermoFisher, 11960-044) containing 10%
428 fetal bovine serum, 1x GlutaMax and 100 μg/ml penicillin–streptomycin. Cells at 70–
429 90% confluency were transfected with equal amounts of luciferase reporter and gene
430 expression plasmids using Lipofectamine 3000 (ThermoFisher). Luciferase activity in the
431 cell lysates was measured using a Dual-Luciferase Reporter Assay System (Promega)
432 according to the manufacturer's protocol. Firefly luciferase activity of MFCS1-*luc2* using
433 a minimum promoter (minP) or *shh* promoter (shh pro) was normalized to *Renilla*
434 luciferase control activity. The mean value of mock samples by the control construct with
435 the minimum promoter was adjusted to 1.0. For statistical analysis, Student's *t*-tests (two-
436 tailed) were applied when equal variance tests were passed.

437

438 **Bisulfite genomic sequencing**

439 Presumptive autopods of hindlimb buds (Tschumi, 1957) from thirty-five wild-type and
440 sixteen MFCS1-GFP Tg (line 1) tadpoles at stage 54 were collected. Forelimb autopods
441 from five wild-type and six MFCS1-GFP Tg (line 1) froglets were collected. Spike
442 regenerates from two MFCS1-GFP Tg (line 1) and two same Tg (line 2) frogs were
443 collected. Then genomic DNA was extracted from these tissue samples. The genomic
444 DNA was treated with sodium bisulfite using an EZ DNA Methylation-Gold Kit
445 following the protocol of the manufacturer (Zymo Research). DNA was amplified by 30
446 cycles of a three-step PCR (98℃ for 10 sec, 60℃ for 30 sec and 68℃ for 30 sec) with
447 MFCS1_BS_Fw and MFCS1_BS_Rv primers (Table S3) using KOD -Multi & Epi-
448 (Toyobo). Each product was cloned into the pANT vector (Nippon Gene) or pGEM-T
449 easy (Promega) and sequenced with M13F-pUC or M13R-pUC primers (Table S3).

450

451 ## ACKNOWLEDGMENTS

452 We thank Yoshiko Yoshizawa and Natsume Sagawa for excellent animal care. We thank
453 Drs. Makoto Asashima, Shuji Takahashi and Yoshio Yaoita for providing the Nigerian
454 line of *X. tropicalis*. We thank Dr. Ikuo Uchiyama for support in gene expression analysis.
455 This work was partially supported by the NIBB Collaborative Research Program to HY
456 (19-451, 20-436, 21-307, 21-401). This work was supported by the National Bio-
457 Resource Project (NBRP) of the MEXT, Japan. We acknowledge Shared Facility Center
458 for Science and Technology, Hirosaki University (SFCST) for confocal microscope
459 observation by FV3000 (Olympus). We thank Dr. Chisato Ushida, Dr. Michiko Sasabe,
460 Shunsuke Hosoi, Misako Saida and Hibiki Yokoyama for their help in using confocal
461 microscopy. We thank Dr. Daisuke Kurita for help in TA cloning. We thank Drs. Gembu
462 Abe and Kazuya Kobayashi for their help in preparation of tungsten needles. We thank
463 Dr. Jose F. de Celis for providing *Xenopus laevis dusp6* cDNA.

464

465 **Competing interests**

466 The authors declare no competing or financial interests.

467

468 **Author contributions**

469 Conceptualization: K.T., H.Y.; Methodology: T.A., N.Y.-K., J.S., Y.K., H.Y.; Validation:
470 T.A., N.Y.-K., H.Y.; Formal analysis: T.A., H.Ogino, H.Y.; Investigation: R.T., T.H., T.A.,
471 S.I., C.Y., S.N., K.I., A.K., H.Ochi, H.Ogino, N.Y.-K., Y.K., H.Y.; Resource: T.A., A.K.,
472 H.Ochi, H.Ogino, N.Y.-K., Y.K., K.T., H.Y.; Writing – original draft preparation: T.A.,
473 H.Ogino, J.S., Y.K., H.Y.; Writing – review and editing: A.K., H.Ochi, H.Ogino, N.Y.-K.,
474 K.T., H.Y.; Visualization: R.T., T.H., T.A., S.I., H.Ogino, N.Y.-K., H.Y.; Supervision:
475 K.T., H.Y.; Project administration: H.Ogino, K.T., H.Y.; Funding acquisition: K.T., H.Y.

476

477 **Funding**

478 H.Y is funded by MEXT and JSPS KAKENHI (grant number 22124005). H.Y. is funded
479 by JSPS KAKENHI (grant number 16H04790, 21K06195). H.Y. is funded by Grant for
480 Basic Science Research Projects from The Sumitomo Foundation. H.Y is funded by
481 Hirosaki University Institutional Research Grant for Young investigators.

482

483 ## REFERENCES

484 **Amano, T., Sagai, T., Tanabe, H., Mizushina, Y., Nakazawa, H. and Shiroishi, T.**
485 (2009). Chromosomal dynamics at the Shh locus: limb bud-specific differential
486 regulation of competence and active transcription. *Dev Cell* **16**, 47-57.
487 **Cameron, J. A. and Fallon, J. F.** (1977). Evidence for polarizing zone in the limb buds
488 of Xenopus laevis. *Dev Biol* **55**, 320-330.
489 **Capellini, T. D., Di Giacomo, G., Salsi, V., Brendolan, A., Ferretti, E., Srivastava,**
490 **D., Zappavigna, V. and Selleri, L.** (2006). Pbx1/Pbx2 requirement for distal
491 limb patterning is mediated by the hierarchical control of Hox gene spatial
492 distribution and Shh expression. *Development* **133**, 2263-2273.
493 **Castro-Mondragon, J. A., Riudavets-Puig, R., Rauluseviciute, I., Lemma, R. B.,**
494 **Turchi, L., Blanc-Mathieu, R., Lucas, J., Boddie, P., Khan, A., Manosalva**
495 **Pérez, N., et al.** (2022). JASPAR 2022: the 9th release of the open-access
496 database of transcription factor binding profiles. *Nucleic Acids Res* **50**, D165-
497 D173.
498 **Dent, J. N.** (1962). Limb regeneration in larvae and metamorphosing individuals of the
499 South African clawed toad. *J Morphol* **110**, 61-77.
500 **Eblaghie, M. C., Lunn, J. S., Dickinson, R. J., Münsterberg, A. E., Sanz-Ezquerro,**
501 **J. J., Farrell, E. R., Mathers, J., Keyse, S. M., Storey, K. and Tickle, C.**
502 (2003). Negative feedback regulation of FGF signaling levels by Pyst1/MKP3 in
503 chick embryos. *Curr Biol* **13**, 1009-1018.
504 **Edgar, R. C.** (2004). MUSCLE: multiple sequence alignment with high accuracy and
505 high throughput. *Nucleic Acids Res* **32**, 1792-1797.
506 **Ekerot, M., Stavridis, M. P., Delavaine, L., Mitchell, M. P., Staples, C., Owens, D.**

507 **M., Keenan, I. D., Dickinson, R. J., Storey, K. G. and Keyse, S. M.** (2008).
508 Negative-feedback regulation of FGF signalling by DUSP6/MKP-3 is driven by
509 ERK1/2 and mediated by Ets factor binding to a conserved site within the
510 DUSP6/MKP-3 gene promoter. *Biochem J* **412**, 287-298.
511 **Endo, T., Tamura, K. and Ide, H.** (2000). Analysis of gene expressions during
512 Xenopus forelimb regeneration. *Dev Biol* **220**, 296-306.
513 **Endo, T., Yokoyama, H., Tamura, K. and Ide, H.** (1997). Shh expression in
514 developing and regenerating limb buds of Xenopus laevis. *Dev Dyn* **209**, 227-
515 232.
516 **Fortriede, J. D., Pells, T. J., Chu, S., Chaturvedi, P., Wang, D., Fisher, M. E.,**
517 **James-Zorn, C., Wang, Y., Nenni, M. J., Burns, K. A., et al.** (2020).
518 Xenbase: deep integration of GEO & SRA RNA-seq and ChIP-seq data in a
519 model organism database. *Nucleic Acids Res* **48**, D776-D782.
520 **Gómez, A. R., López-Varea, A., Molnar, C., de la Calle-Mustienes, E., Ruiz-**
521 **Gómez, M., Gómez-Skarmeta, J. L. and de Celis, J. F.** (2005). Conserved
522 cross-interactions in Drosophila and Xenopus between Ras/MAPK signaling and
523 the dual-specificity phosphatase MKP3. *Dev Dyn* **232**, 695-708.
524 **Han, M., Yang, X., Taylor, G., Burdsal, C. A., Anderson, R. A. and Muneoka, K.**
525 (2005). Limb regeneration in higher vertebrates: developing a roadmap. *Anat*
526 *Rec B New Anat* **287**, 14-24.
527 **Harfe, B. D., Scherz, P. J., Nissim, S., Tian, H., McMahon, A. P. and Tabin, C. J.**
528 (2004). Evidence for an expansion-based temporal Shh gradient in specifying
529 vertebrate digit identities. *Cell* **118**, 517-528.
530 **Hayashi, S., Kawaguchi, A., Uchiyama, I., Kawasumi-Kita, A., Kobayashi, T.,**
531 **Nishide, H., Tsutsumi, R., Tsuru, K., Inoue, T., Ogino, H., et al.** (2015).
532 Epigenetic modification maintains intrinsic limb-cell identity in Xenopus limb
533 bud regeneration. *Dev Biol* **406**, 271-282.
534 **Hirsch, N., Zimmerman, L. B., Gray, J., Chae, J., Curran, K. L., Fisher, M.,**
535 **Ogino, H. and Grainger, R. M.** (2002). Xenopus tropicalis transgenic lines and
536 their use in the study of embryonic induction. *Dev Dyn* **225**, 522-535.
537 **Igawa, T., Watanabe, A., Suzuki, A., Kashiwagi, A., Kashiwagi, K., Noble, A.,**
538 **Guille, M., Simpson, D. E., Horb, M. E., Fujii, T., et al.** (2015). Inbreeding
539 Ratio and Genetic Relationships among Strains of the Western Clawed Frog,
540 Xenopus tropicalis. *PloS One* **10**, e0133963.
541 **Imokawa, Y. and Yoshizato, K.** (1997). Expression of Sonic hedgehog gene in
542 regenerating newt limb blastemas recapitulates that in developing limb buds.
543 *Proc Natl Acad Sci U S A* **94**, 9159-9164.
544 **Joven, A., Elewa, A. and Simon, A.** (2019). Model systems for regeneration:
545 salamanders. *Development* **146**.
546 **Karolchik, D., Baertsch, R., Diekhans, M., Furey, T. S., Hinrichs, A., Lu, Y. T.,**
547 **Roskin, K. M., Schwartz, M., Sugnet, C. W., Thomas, D. J., et al.** (2003).
548 The UCSC Genome Browser Database. *Nucleic Acids Res* **31**, 51-54.
549 **Kawakami, Y., Rodríguez-León, J., Koth, C. M., Büscher, D., Itoh, T., Raya, A.,**
550 **Ng, J. K., Esteban, C. R., Takahashi, S., Henrique, D., et al.** (2003). MKP3
551 mediates the cellular response to FGF8 signalling in the vertebrate limb. *Nat*
552 *Cell Biol* **5**, 513-519.
553 **Kroll, K. L. and Amaya, E.** (1996). Transgenic Xenopus embryos from sperm nuclear

554 transplantations reveal FGF signaling requirements during gastrulation.
555 *Development* **122**, 3173-3183.
556 **Lettice, L. A., Heaney, S. J., Purdie, L. A., Li, L., de Beer, P., Oostra, B. A., Goode,**
557 **D., Elgar, G., Hill, R. E. and de Graaff, E.** (2003). A long-range Shh enhancer
558 regulates expression in the developing limb and fin and is associated with
559 preaxial polydactyly. *Hum Mol Genet* **12**, 1725-1735.
560 **Lettice, L. A., Williamson, I., Wiltshire, J. H., Peluso, S., Devenney, P. S., Hill, A.**
561 **E., Essafi, A., Hagman, J., Mort, R., Grimes, G., et al.** (2012). Opposing
562 functions of the ETS factor family define Shh spatial expression in limb buds
563 and underlie polydactyly. *Dev Cell* **22**, 459-467.
564 **Muneoka, K., Holler-Dinsmore, G. and Bryant, S. V.** (1986). Intrinsic control of
565 regenerative loss in Xenopus laevis limbs. *J Exp Zool* **240**, 47-54.
566 **Nieuwkoop, P. D. and Faber, J.** (1994). *Normal Table of Xenopus laevis (Daudin).*
567 New York: Garland Publishing.
568 **Nuñez, J. K., Chen, J., Pommier, G. C., Cogan, J. Z., Replogle, J. M., Adriaens, C.,**
569 **Ramadoss, G. N., Shi, Q., Hung, K. L., Samelson, A. J., et al.** (2021).
570 Genome-wide programmable transcriptional memory by CRISPR-based
571 epigenome editing. *Cell* **184**, 2503-2519.e17.
572 **Ogino, H. and Ochi, H.** (2009). Resources and transgenesis techniques for functional
573 genomics in Xenopus. *Dev Growth Differ* **51**, 387-401.
574 **Otsuki, L. and Tanaka, E. M.** (2022). Positional Memory in Vertebrate Regeneration:
575 A Century's Insights from the Salamander Limb. *Cold Spring Harb Perspect*
576 *Biol* **14**.
577 **Riddle, R. D., Johnson, R. L., Laufer, E. and Tabin, C.** (1993). Sonic hedgehog
578 mediates the polarizing activity of the ZPA. *Cell* **75**, 1401-1416.
579 **Roy, S. and Gardiner, D. M.** (2002). Cyclopamine induces digit loss in regenerating
580 axolotl limbs. *J Exp Zool* **293**, 186-190.
581 **Sagai, T., Hosoya, M., Mizushina, Y., Tamura, M. and Shiroishi, T.** (2005).
582 Elimination of a long-range cis-regulatory module causes complete loss of limb-
583 specific Shh expression and truncation of the mouse limb. *Development* **132**,
584 797-803.
585 **Sagai, T., Masuya, H., Tamura, M., Shimizu, K., Yada, Y., Wakana, S., Gondo, Y.,**
586 **Noda, T. and Shiroishi, T.** (2004). Phylogenetic conservation of a limb-
587 specific, cis-acting regulator of Sonic hedgehog (Shh). *Mamm Genome* **15**, 23-
588 34.
589 **Satoh, A., Endo, T., Abe, M., Yakushiji, N., Ohgo, S., Tamura, K. and Ide, H.**
590 (2006). Characterization of Xenopus digits and regenerated limbs of the froglet.
591 *Dev Dyn* **235**, 3316-3326.
592 **Suzuki, M., Hayashi, T., Inoue, T., Agata, K., Hirayama, M., Shigenobu, S.,**
593 **Takeuchi, T., Yamamoto, T. and Suzuki, K. T.** (2018). Cas9
594 ribonucleoprotein complex allows direct and rapid analysis of coding and
595 noncoding regions of target genes in Pleurodeles waltl development and
596 regeneration. *Dev Biol* **443**, 127-136.
597 **Suzuki, M., Satoh, A., Ide, H. and Tamura, K.** (2005). Nerve-dependent and -
598 independent events in blastema formation during Xenopus froglet limb
599 regeneration. *Dev Biol* **286**, 361-375.
600 **Suzuki, M., Yakushiji, N., Nakada, Y., Satoh, A., Ide, H. and Tamura, K.** (2006).

601 Limb regeneration in Xenopus laevis froglet. *ScientificWorldJournal* **6 Suppl 1**,
602 26-37.
603 **Torok, M. A., Gardiner, D. M., Izpisúa-Belmonte, J. C. and Bryant, S. V.** (1999).
604 Sonic hedgehog (shh) expression in developing and regenerating axolotl limbs. *J*
605 *Exp Zool* **284**, 197-206.
606 **Tschumi, P. A.** (1957). The growth of the hindlimb bud of Xenopus laevis and its
607 dependence upon the epidermis. *J Anat* **91**, 149-173.
608 **Wingender, E.** (2008). The TRANSFAC project as an example of framework
609 technology that supports the analysis of genomic regulation. *Brief Bioinform* **9**,
610 326-332.
611 **Yakushiji, N., Suzuki, M., Satoh, A., Sagai, T., Shiroishi, T., Kobayashi, H., Sasaki,**
612 **H., Ide, H. and Tamura, K.** (2007). Correlation between Shh expression and
613 DNA methylation status of the limb-specific Shh enhancer region during limb
614 regeneration in amphibians. *Dev Biol* **312**, 171-182.
615 **Yakushiji, N., Yokoyama, H. and Tamura, K.** (2009). Repatterning in amphibian
616 limb regeneration: A model for study of genetic and epigenetic control of organ
617 regeneration. *Semin Cell Dev Biol* **20**, 565-574.
618 **Yokoyama, H., Endo, T., Tamura, K., Yajima, H. and Ide, H.** (1998). Multiple digit
619 formation in Xenopus limb bud recombinants. *Dev Biol* **196**, 1-10.
620 **Yoshida, K., Urase, K., Takahashi, J., Ishii, Y. and Yasugi, S.** (1996). Mucus-
621 associated antigen in epithelial cells of the chicken digestive tract:
622 developmental change in expression and implications for morphogenesis-
623 function relationships. *Dev. Growth Differ.* **38**, 185-192.
624

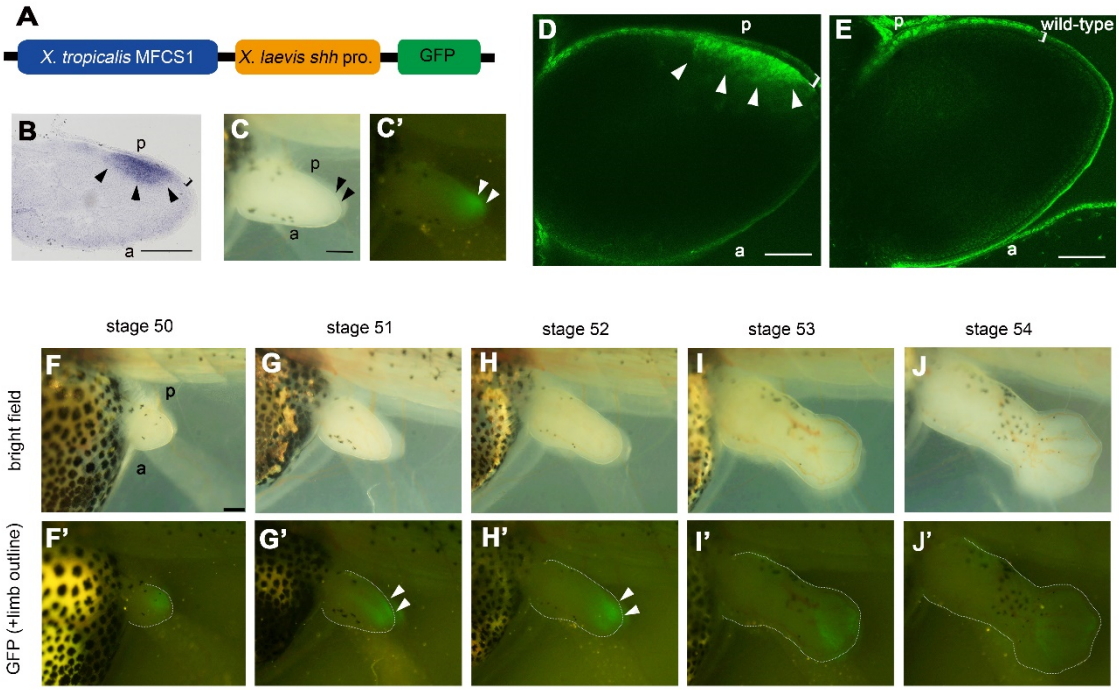

625

626 **Fig. 1. MFCS1-GFP expression coincides with *shh* expression in a developing limb**
627 **bud.** (A) The MFCS1-GFP transgene. (B) *shh* expression at stage 52. (C, C') A limb bud
628 of an MFCS1-GFP tadpole at stage 51. Bright-field (C) and fluorescent (C') images. (D,
629 E) Optical-section images by confocal microscopy of the limb bud of an MFCS1-GFP
630 (D) and that of a wild-type tadpole at stage 51. Bright-field (F-J) and fluorescent (F'-J')
631 images of the limb bud of the same MFCS1-GFP tadpole. Limb buds are outlined by
632 dotted lines in the fluorescent images. All of the MFCS1-GFP tadpoles shown are line 1.
633 a, anterior: p, posterior. Arrowheads, *shh* (B) or GFP expression (D, E, G', H') at the
634 posterior side: Bracket, the epidermal cell layer. Bars = 100 μm for (B, D ,E) and 200 μm
635 for (C, C', F-J, F'-J').

636

637

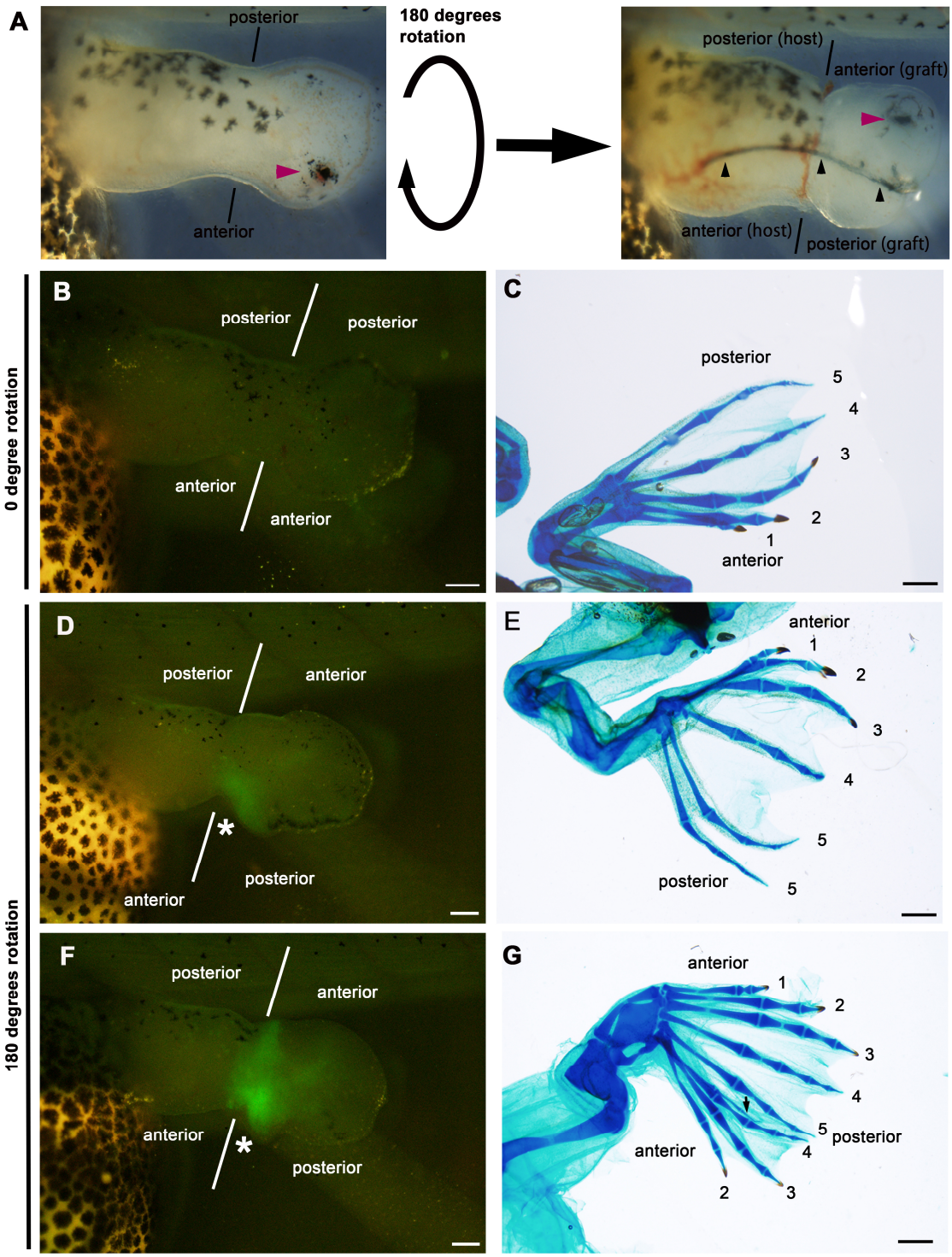

638

639 **Fig. 2. MFCS1-GFP expression precedes limb duplication along the AP axis in 180°**
640 **rotated limb buds.** (A) 180° rotation of a limb bud at stage 53. A magenta arrowhead, a
641 Nile blue particle: Black arrowheads, a tungsten pin. (B, C) A 0° rotated limb bud at 6
642 days after grafting (B) and the resultant normal limb formation (C). (D-G) 180° rotated

643 limb buds. Rotated limb buds at 6 days after grafting (D,F) resulted in supernumerary
644 limb formation (E,G). A pair of lines, the host-graft boundary: An asterisk, ectopic GFP:
645 An Arabic number, the digit identity: A black arrow, an unidentifiable digit. Bars = 200
646 μm for (B, D, F) and 1 mm for (C, E, F).
647

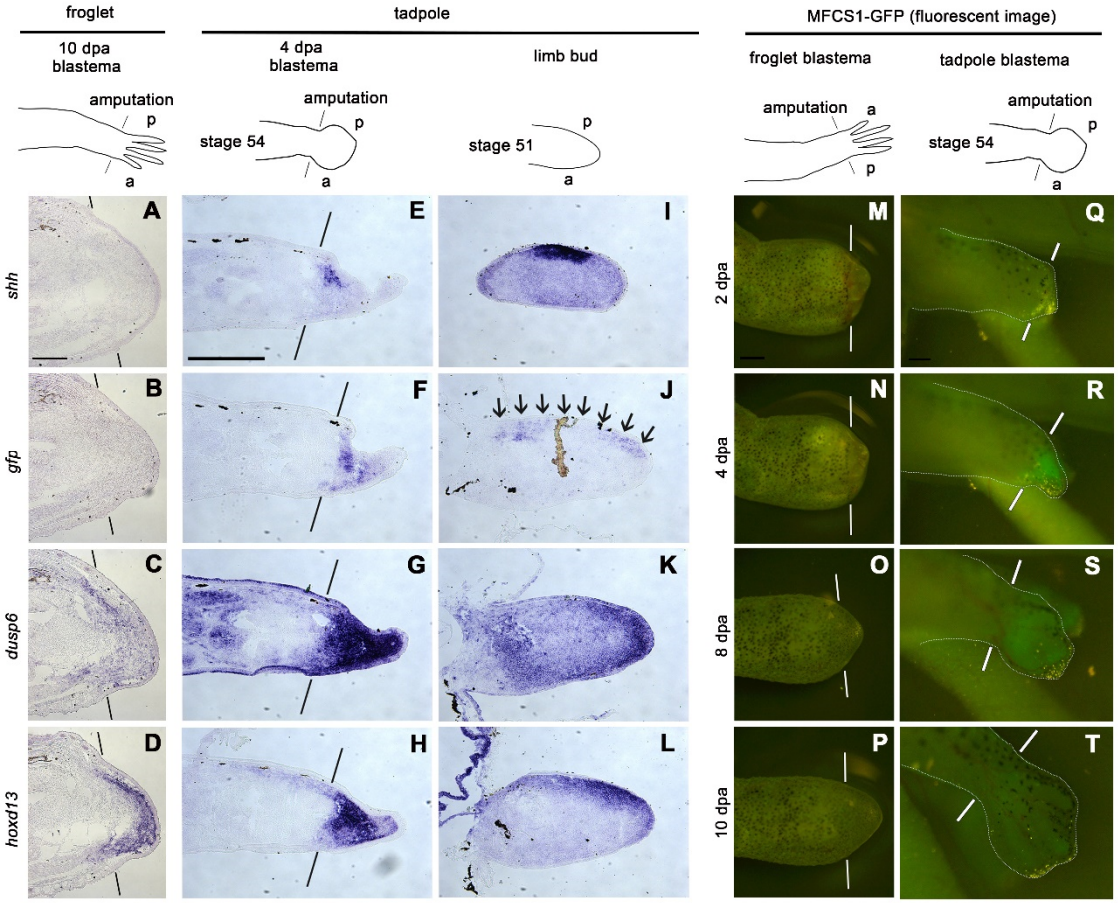

Fig. 3. Comparison of gene expression patterns and MFCS1-GFP expression pattern in a regenerating limb in a young tadpole and a froglet. (A-D) Adjacent sections of a blastema of a froglet. n=5 of 5 blastemas (line 1). (E-H) Adjacent sections of a blastema of a tadpole. n=9 of 9 (line 1) and 6 of 6 blastemas (line 2), respectively. (I-L) Adjacent sections of a limb bud. n=10 of 10 (line 1) and 6 of 6 limb buds (line 2), respectively. (M-P) A blastema of a froglet of line 1. See also Fig. S3. (Q-T) A blastema of a tadpole of line 1. The blastema and the stump are outlined by a dotted line. See also Fig. S2. a, anterior: p, posterior. A pair of lines, the amputation level: Arrows, *gfp* expression at the posterior side. All pictures shown in Fig. 3 are samples of line 1. Bar = 200 μm for (A-L, Q-T) and 500 μm for (M-P).

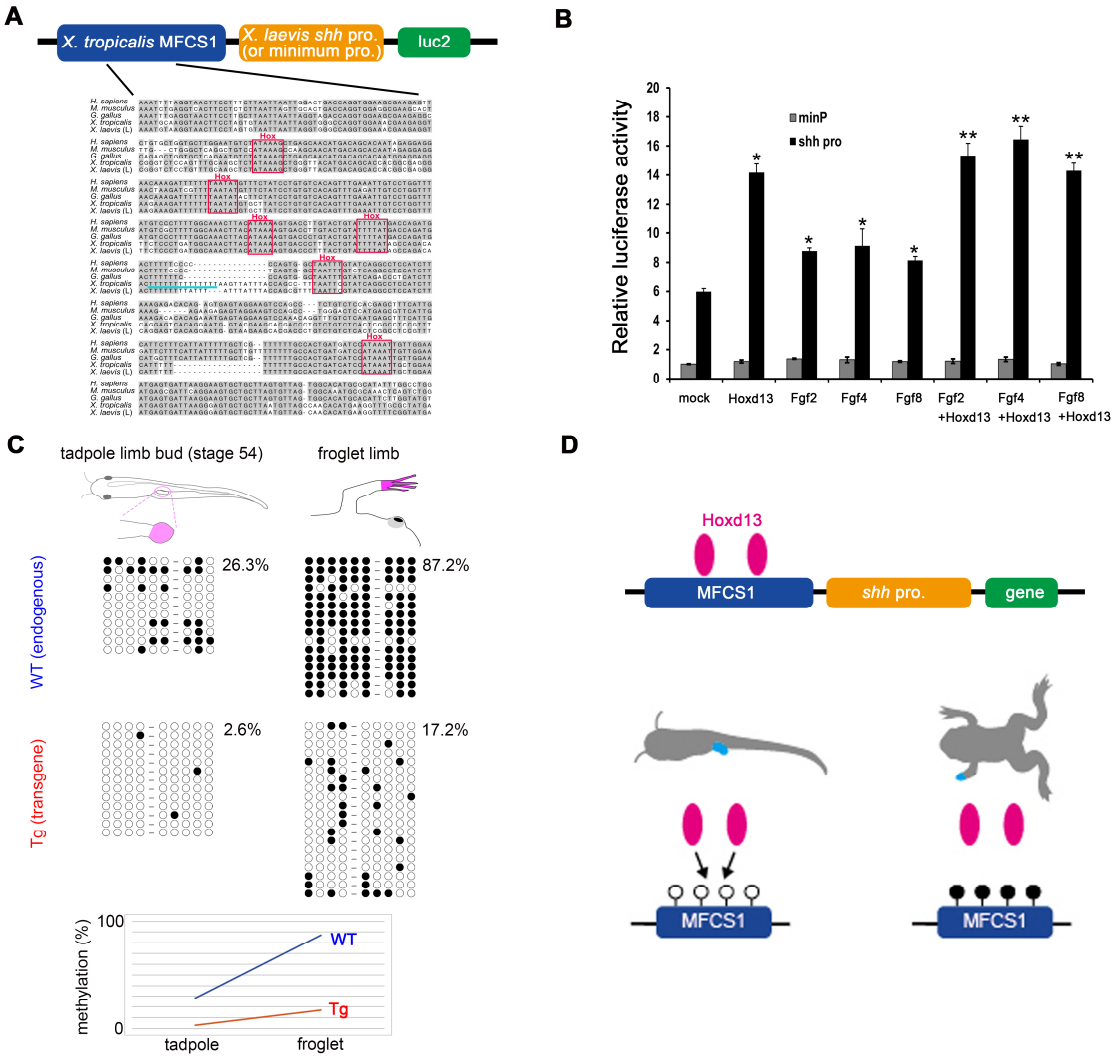

Fig. 4. Transactivation and DNA methylation of *Xenopus* MFCS1 enhancer. (A) Upper: Map of MFCS1-*luc2* for assays in (B). Lower: Alignment of MFCS1 highly conserved sequences. Nucleotides identical in more than two sequences are shaded. Conserved Hox-binding motifs are boxed. A light bule line underlies the 14-thymidine repeat. (B) Normalized luciferase activity. Error bars, standard deviation from the mean (n=3). *Significant increase from mock (p<0.01). **Significant increase in Fgf2+Hoxd13, Fgf4+Hoxd13 and Fgf8+Hoxd13 from sole Fgf2, Fgf4 and Fgf8, respectively (p<0.01). (C) Methylation pattern of endogenous and transgene MFCS1 (line 1). Samples were obtained from the autopod (pink). Circles correspond to nine CpG sites (Fig. S6). Lower: Increases in average methylation rate of the MFCS1 after metamorphosis. (D) Model for epigenetic silencing of gene expression. Hoxd13 activates hypomethylated MFCS1 and results in transcription of a gene (left). However, Hoxd13 is

674 unable to activate highly methylated MFCS1 and results in inactive transcription (right).

675

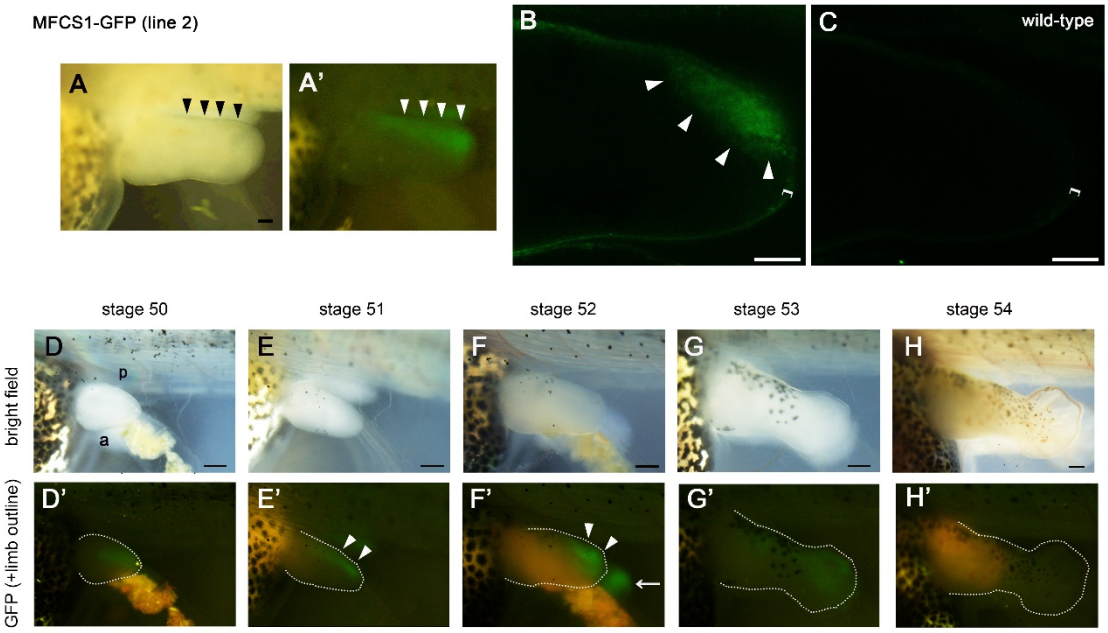

676

677 **Fig. S1. MFCS1-GFP expression pattern was recapitulated in line 2.** (A) A developing
678 limb bud of an MFCS1-GFP Tg tadpole of line 2 at stage 52. Bright-field (A) and
679 fluorescent (A') images of the same limb bud. (B, C) Optical-section images by confocal
680 microscopy of the limb bud of an MFCS1-GFP Tg tadpole of line 2 (B) and a wild-type
681 tadpole (C) at stage 52. GFP expression was detected in the posterior side mesenchyme
682 specifically in the MFCS1-GFP Tg tadpole. Bright field (D-H) and fluorescent (D'-H')
683 images of the limb bud of the same Tg tadpole of line 2. Limb buds are outlined by dotted
684 lines. GFP expression was detected in the posterior side of limb buds at stage 51-52 and
685 then gradually diminished. a, anterior: p, posterior. Arrowheads, GFP expression (A, A',
686 B, E', F') at the posterior side of the limb buds: Bracket, the epidermal cell layer: A pair
687 of lines, the amputation level. Bars = 100 μm for (A, B, C), 200 μm for (D-H, D'-H').

688

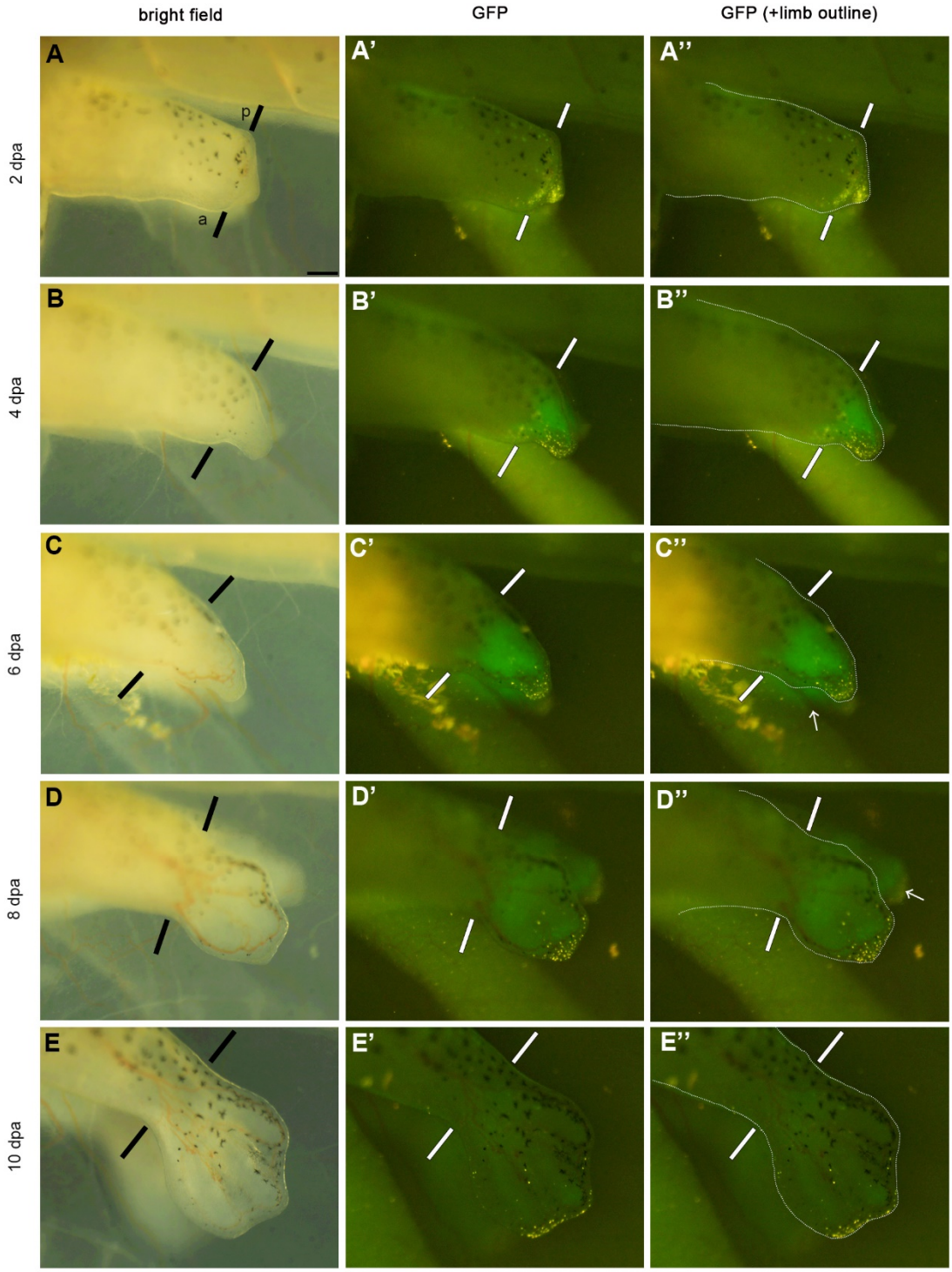

689

690 **Fig. S2. Spatio-temporal expression pattern of MFCS1-GFP in a regenerating limb**
691 **of a young tadpole.** All of the pictures are focused on a limb blastema of the same tadpole
692 (identical to Fig. 3Q-T) of line 1. Left and right limb buds were amputated at the
693 presumptive ankle level of a stage 54 tadpole. GFP fluorescence was distributed

694 throughout the regenerating limb blastema at 4 dpa and 6 dpa. (A'', B'', C'', D'', E''')
695 Limb blastemas and stumps are outlined by dotted lines. n=16 of 16 blastemas from a
696 total of ten MFCS1-GFP tadpoles of line 1 and 6 of 6 blastemas from a total of three
697 MFCS1-GFP tadpoles of line 2, respectively. A pair of lines, the amputation level:
698 Arrows, GFP fluorescence of the contralateral right limb blastemas: a, anterior: p,
699 posterior. Bar = 200 μm.
700

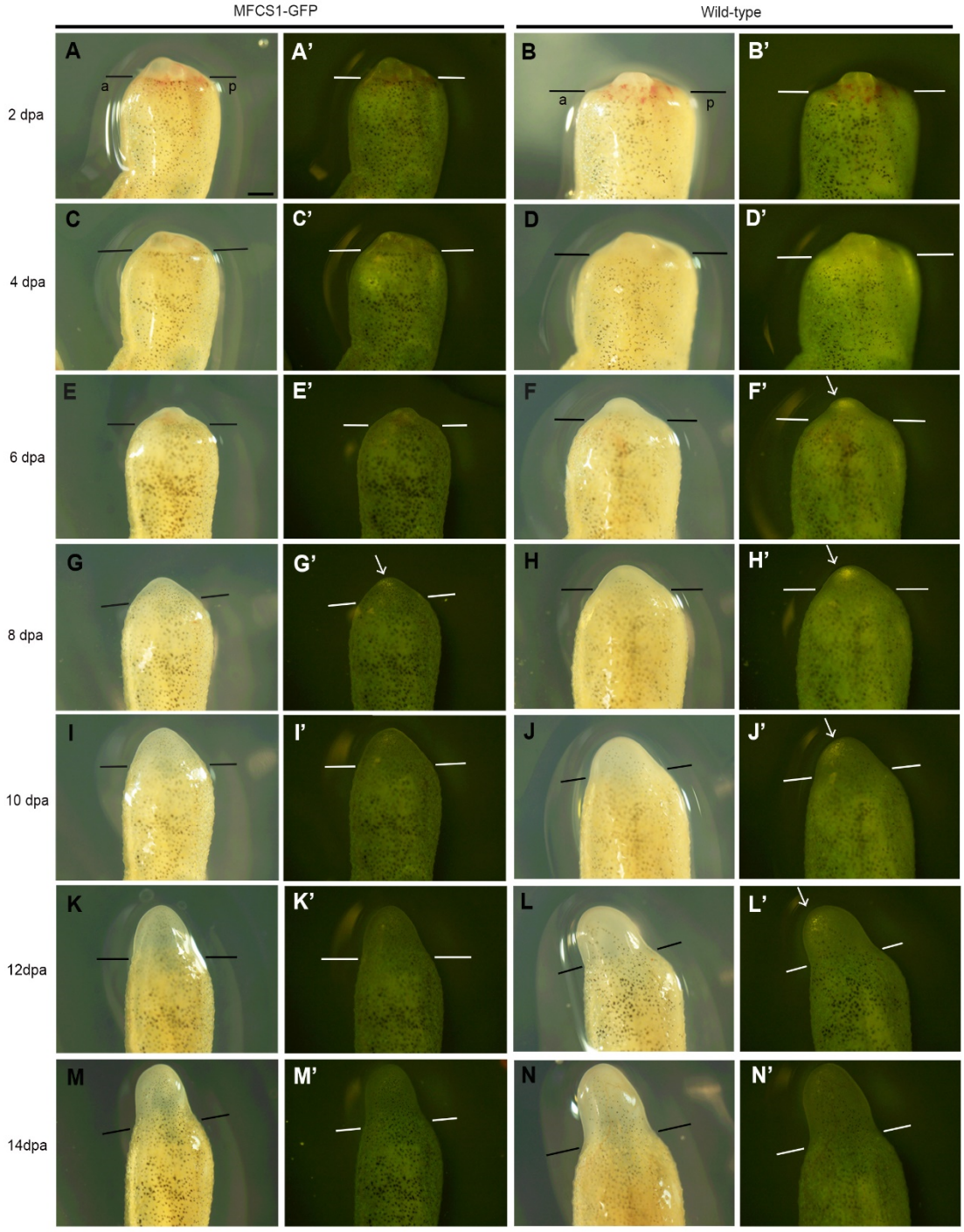

701

702 **Fig. S3. MFCS1-GFP expression is inactive in a limb blastema of a froglet.** A blastema
703 of the same froglet of line 1 (left two columns; identical to Fig. 3M-N) and a blastema of
704 the same wild-type froglet (right two columns) from 2 dpa to 14 dpa. No specific GFP
705 fluorescence was observed in the blastema of the Tg froglet at any timepoint. n=4 of 4
706 blastemas from a total of four froglets of line 1, 6 of 6 blastemas from a total of four

707 froglets of line 2 and 8 of 8 blastemas from a total of six wild-type froglets as controls,
708 respectively. A pair of lines, the amputation level: An arrow, non-specific fluorescence
709 commonly observed both in the Tg froglet and wild-type one: a, anterior: p, posterior.
710 Bar = 500 μm.
711

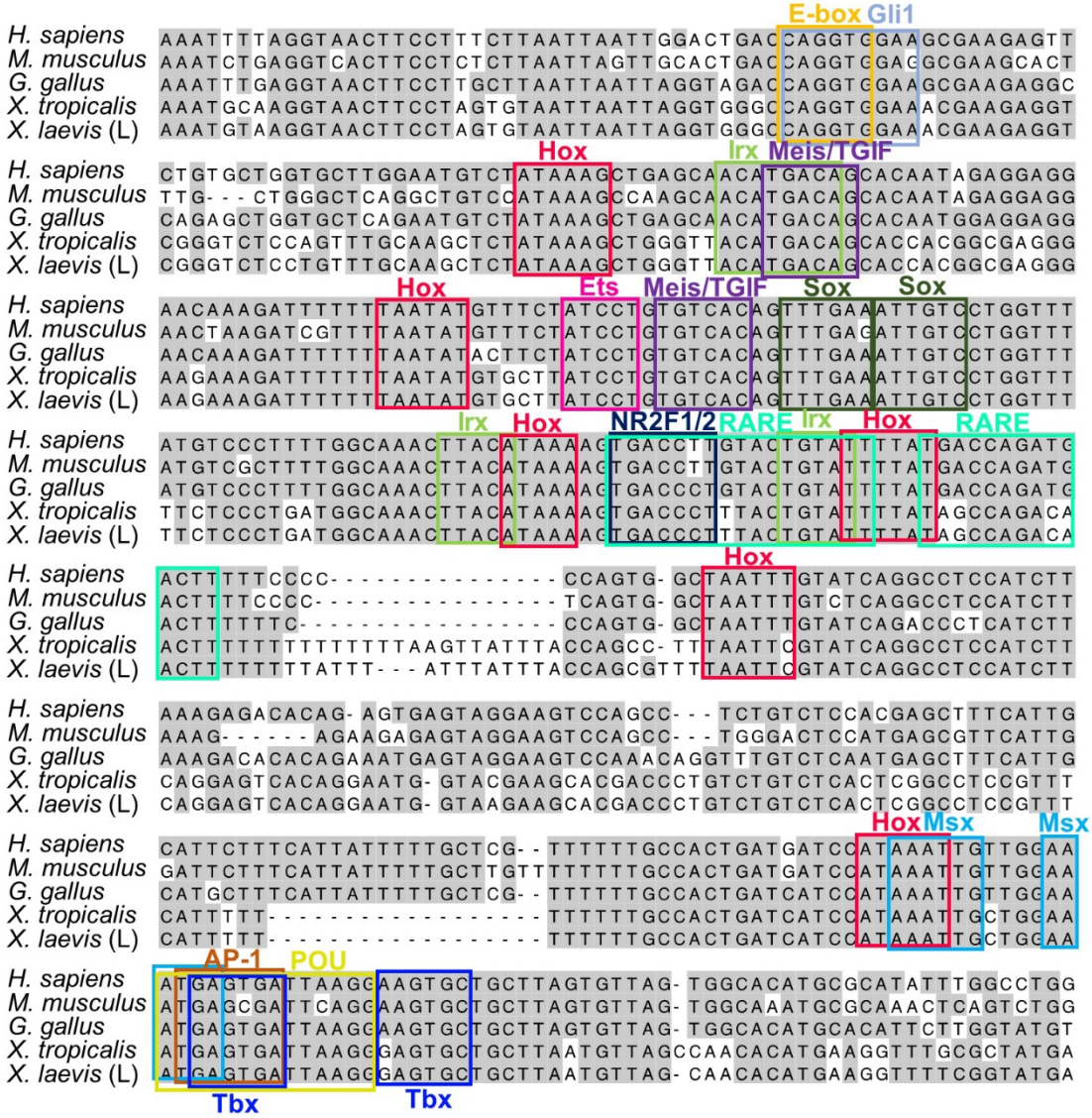

712

713 **Fig. S4. Alignment of MFCS1 highly conserved sequences (identical sequences**
714 **shown in Fig. 4A) from the human, mouse, chick, *X. tropicalis* and *X. laevis*.**
715 Nucleotides identical in more than two sequences are shaded in grey. Conserved
716 transcription factor-binding motifs (Hox and other transcription factors) are boxed.

717

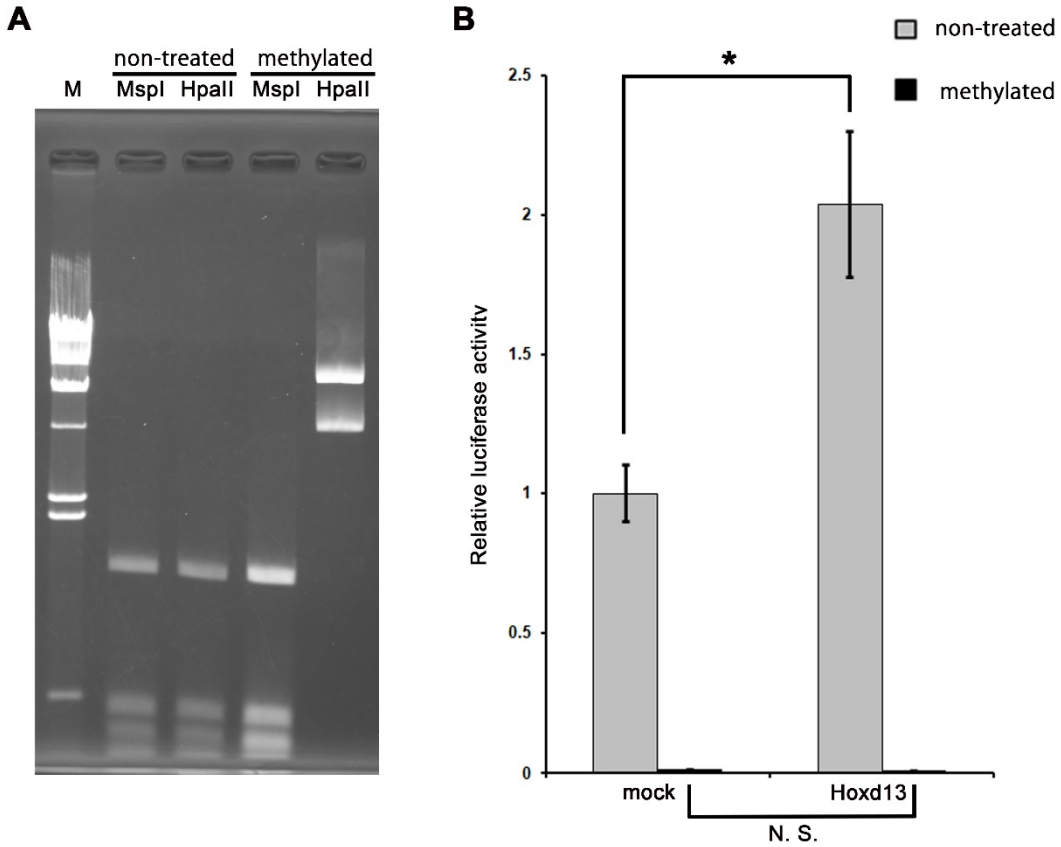

718

719 **Fig. S5. DNA methylation suppresses the response of MFCS1 to Hoxd13 *in vitro*.**
720 (A) Methylation-sensitive restriction digestion visualized by agarose gel
721 electrophoresis. Plasmid DNA of the MFCS1-*shh* promoter-*luc2* reporter was treated
722 with CpG methyltransferase (M. SssI, NEB) according to the manufacturer's protocol.
723 Methylation efficiency of the plasmid DNA was evaluated by digestion with
724 methylation-sensitive (HpaII) and -insensitive (MspI) restriction enzymes. The CpG
725 methylation prohibited the digestion of the plasmid DNA specifically with HpaII. M,
726 λ/HindIII marker. (B) Luciferase activity in NIH3T3 cells transfected with the
727 methylated or non-treated MFCS1-*luc2* reporter constructs and the *Hoxd13* expression
728 construct. The mean value of luciferase activity in cells transfected with the non-treated
729 reporter and mock expression constructs was set to 1.0. Error bars: standard deviation
730 from the mean (n=3). While a significant increase of *Hoxd13*-induced luciferase activity
731 was observed in cells transfected with the unmethylated reporter construct (*$p<0.01$),
732 being consistent with Fig. 4B, there was no significant increase in cells transfected with
733 the methylated reporter construct despite *Hoxd13* expression. N. S., not significant.

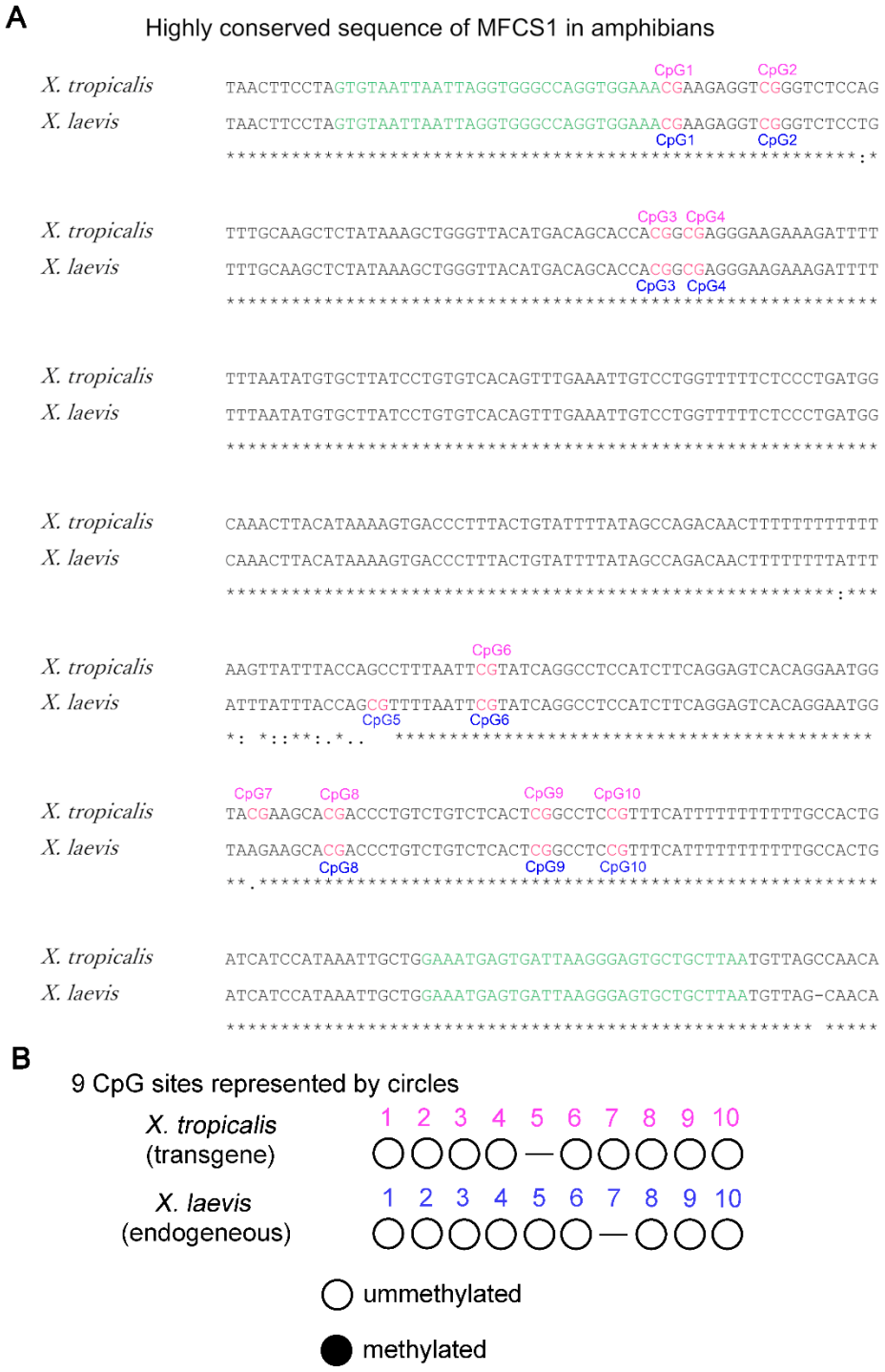

Fig. S6. *X. tropicalis* and *X. laevis* have 9 CpG sites in the highly conserved sequence of MFCS1. (A) Alignment of MFCS1 highly conserved sequences between *X. tropicalis* and *X. laevis*. Green letters correspond to MFCS1_BS_Fw and MFCS1_BS_Rv primers for bisulfite sequencing (see also Table S3). (B) Open and black circles represent unmethylated and methylated CpG sites, respectively.

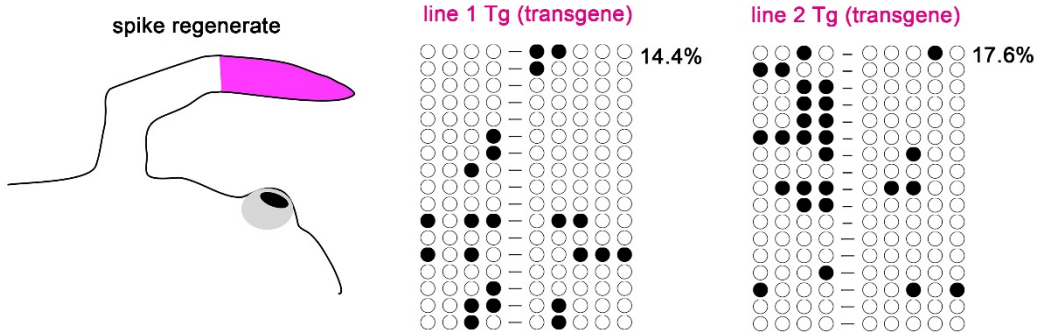

Fig. S7. Methylation pattern of MFCS1 in a spike regenerate after limb regeneration of a froglet. After limb blastemas of froglets completed spike regeneration, regenerate samples (pink) were obtained from line 1 and line 2 Tg frogs.

Table S1. Rate of germline transmission and activity of MFCS1-GFP

G0	N1	N2
	GFP+/ total	GFP+/ total
line 1	195/368 (53%)	70/172 (41%)
line 2	79/180 (44%)	not applicable

Table S2. Supernumerary limb formation and ectopic GFP in rotated limb buds

180° rotated limb buds

Sample	No. of original digits	No. of supernumerary digits	No. of digits (total)	Is there ectopic GFP?	Figure
1	5	2	7	Yes	-
2	5	2	7	Yes	-
3	5	2	7	Yes	-
4	5	2	7	Yes	-
5	5	4	9	Yes	Fig. 2F, G
6	5	2	7	Yes	-
7	5	1	6	Yes	Fig. 2D, E
8	5	0	5	No	-
9	5	0	5	No	-
10	5	0	5	No	-
11	5	2	7	Yes	-

0° rotated limb buds (controls)

Sample	No. of original digits	No. of supernumerary digits	No. of digits (total)	Is there ectopic GFP?	Figure
1	5	0	5	No	Fig. 2B, C
2	5	0	5	No	-
3	5	0	5	No	-
4	5	0	5	No	-
5	5	0	5	No	-
6	5	0	5	No	-
7	5	0	5	No	-
8	5	0	5	No	-
9	5	0	5	No	-
10	5	0	5	No	-
11	5	5	10	Yes	-
12	5	3	8	Yes	-

Table S3. Primers for genomic- and RT-PCR

name	Sequence (5’ -> 3’)	note
xtMFCS1-Fw	ACTGTAACCAGTGAAAATCATCAGTCATGAATATC	transgene
xtMFCS1-Rv	TGGCCTAGTTCATAGACATTAATTATTTTTCTATGGG	transgene
xtM1-Acc65I-Fw	ttggtaccTTCAAATGATGGATTTTCATATTATAA	Luc reporter
xtM1-XhoI-Rv	ggctcgaGACCATGAAGGCACCCTAATACT	Luc reporter
xlpS-XhoI-Fw	ggctcgAGTGACACCGTGGAAGCCTTTATTATC	Luc reporter
xlpS-NcoI-Rv	ggccatggtGTCCGAGCGAAGCCAATTACATCA	Luc reporter
Fgf2_cds_F1	GCCATGGCTGCCAGCGGCATCACC	Gene Expression
Fgf2_cds_R1	TCAGCTCTTAGCAGACATTGGAAG	Gene Expression
Fgf4_cds_F1	CCGGGATGGCGAAACGCGGGCCGA	Gene Expression
Fgf4_cds_R1	TCACAGTCTAGGAAGGAAGTGGGT	Gene Expression
Fgf8_cds_F1	GACCCCGCTCGGGCTCTCAGTGCT	Gene Expression
Fgf8_cds_R1	CTATCGGGGCTCCGGGGCCCAAGT	Gene Expression
Hoxd13-F	ATGAGCCGCTCGGGGACTTG	Gene Expression
Hoxd13-R	TCAGGAGACAGTGTCTTTGA	Gene Expression
MFCS1_BS_Fw	GTGTAATTAATTAGGTGGGyyAGGTGGAAA	Bisulfite sequencing
MFCS1_BS_Rv	TTAArCArCACTCCCTTAATCACTCATTTC	Bisulfite sequencing
M13F-pUC	GTTTTCCCAGTCACGAC	Bisulfite sequencing
M13R-pUC	CAGGAAACAGCTATGAC	Bisulfite sequencing